

Germacrone derivatives: synthesis, biological activity, molecular docking studies and molecular dynamics simulations

Jie Wu¹, Yu Feng¹, Chao Han¹, Wu Huang³, Zhibin Shen⁴, Mengdie Yang², Weiqiang Chen², Lianbao Ye¹

¹School of Pharmacy, Guangdong Pharmaceutical University, Guangzhou 510006, China

²School of Basic Courses, Guangdong Pharmaceutical University, Guangzhou 510006, China

³Inspection and Quarantine Technology Center of Zhanjiang Entry-Exit Inspection and Quarantine Bureau, Zhanjiang 524001, China

⁴School of Traditional Chinese Medicine, Guangdong Pharmaceutical University, Guangzhou 510006, China

Correspondence to: Lianbao Ye, email: yelb7909@163.com

Keywords: germacrone derivative, biological activity, c-Met kinase, molecular docking, molecular dynamics simulations

Received: September 30, 2016

Accepted: January 13, 2017

Published: January 27, 2017

ABSTRACT

Germacrone is one of the major bioactive components in the *Curcuma zedoaria* oil product, which is extracted from *Curcuma zedoaria* Roscoe, known as *zedoary*. The present study designed some novel germacrone derivatives based on combination principles, synthesized these compounds, and investigated their inhibitions on Bel-7402, HepG2, A549 and HeLa cells. Meanwhile, the study evaluated inhibitions of these derivatives on c-Met kinase, which has been detected in a number of cancers. The results suggested that the majority of the compounds showed stronger inhibitory effect on cancers and c-Met kinase than germacrone. Furthermore, our docking experiments analyzed the results and explained the molecular mechanism. Molecular dynamics simulations were then applied to perform further evaluation of the binding stabilities between compounds and their receptors.

INTRODUCTION

Rhizoma Curcuma belongs to the *Zingiberacea* family, which is composed of about 70 species of rhizomatous herbs at home and abroad, with approximately 20 species existing in China. In China, it is traditionally used for the treatment of dyspepsia, flatulence, menstrual disorders, fever, and cough [1]. *Zedoary's* extract have analgesic, antitumor, antimicrobial, and antiallergic activity [2–6]. Germacrone is a main bioactive constituent found in *Zedoary* oil product which is extracted from *Curcuma zedoaria* Roscoe [7]. The Germacrone (Figure 1) presents extensive bioactivities including antiulcer, antiinflammatory, depressant, vasodilator, antibacterial, choleric, antitussive, antitumor, antifeedant, antifungal and hepatoprotector effects [8–10].

The c-Met signaling pathway plays imperative roles in embryogenesis and early development; whereas c-Met is expressed by most carcinomas and its elevated expression relative to normal tissue has been detected in a number of cancers [11–13]. Activation of the HGF/c-Met signaling pathway has been shown to lead to a wide array

of cellular responses including motility, survival, scattering, wound healing, invasion, angiogenesis, proliferation, tissue regeneration and branching morphogenesis [14–16]. Therefore, c-Met has become an attractive target of antitumor therapy.

References reported that carboxylic esters, especially aromatic esters, had strong anticancer activity. In the present study, carboxylic esters were introduced to germacrone to obtain novel germacrone derivatives (3a–3e) (Figure 2) based on the combination principles. It is hoped that introduction of carboxylic esters can increase anticancer activity of germacrone. Hopefully, it can absorb and distribute to various tissues quickly.

In the present study, we synthesized these compounds and evaluated their inhibitions on Bel-7402, HepG2, A549 and HeLa cells. Meanwhile, the study investigated inhibition of these derivatives on c-Met kinase, which has been over-expressed in a number of cancers. Further, the molecular mechanisms of these compounds to c-Met kinase were explained by docking experiments. The further evaluation of the binding stabilities between compounds and their receptors were performed by molecular dynamics simulations.

RESULTS AND DISCUSSION

Chemistry

The target compounds (2, 3a–3e) were prepared according to Scheme 1. The (3*E*,7*E*)-3,7-dimethyl-10-(propan-2-ylidene)cyclodeca-3,7-dien-1-yl-acetate (3a), (3*E*,7*E*)-3,7-dimethyl-10-(propan-2-ylidene)cyclodeca-3,7-dien-1-yl-4-methylbenzoate(3b), (3*E*,7*E*)-3,7-dimethyl-10-(propan-2-ylidene)cyclodeca-3,7-dien-1-yl-3-methylbenzoate(3c), (3*E*,7*E*)-3,7-dimethyl-10-(propan-2-ylidene)cyclodeca-3,7-dien-1-yl-4-(trifluoromethyl) benzoate (3d), (Z)-(3*E*,7*E*)-3,7-dimethyl-10-(propan-2-ylidene)cyclodeca-3,7-dien-1-yl-3-phenylacrylate (3e) were obtained via DMAP/DCC esterification reaction with yields of 67%, 62%, 47%, 53%, 60%. This reaction was carried out by using dry DCM or acetonitrile as a solvent, DCC as a dehydrator and DMAP as a catalyst and can provide a range of applicability. Due to the distinct difference in polarity, these compounds can be separated easily by silica gel column chromatography. Structural modification of germacrone and a systematic study revealed that the 8-hydroxy might be further optimization studies and a range of substituent would be suitable for this position.

The derivatives were characterized by ¹H NMR, ¹³C NMR, elemental analyses and EI-MS. The analytical data for target compounds can be seen from Experimental and ¹³C NMR and EI-MS gave information about carbon atoms and all the ion peaks corresponding to molecular weight of confirmed novel compounds.

(3*E*,7*E*)-3,7-dimethyl-10-(propan-2-ylidene)cyclodeca-3,7-dienol (2) Yield: 84%, ¹H NMR (400 MHz, CDCl₃) δ 5.29 (dd, J = 11.1, 9.6 Hz, 1H), 5.2–5.1 (m, 1H), 4.4 (dd, J = 5.4, 1.9 Hz, 1H), 2.6 (dd, J = 12.6, 11.3 Hz, 1H), 2.6–2.5 (m, 1H), 2.5 (d, J = 1.9 Hz, 1H), 2.4 (m, 1H), 2.4–2.3 (m, 1H), 2.32 (m, 1H), 2.31–2.25 (m, 2H), 1.7 (s, 6H), 1.57 (s, 3H), 1.55 (s, 3H). ¹³C NMR(100MHz, (D₆) DMSO) δ 138.3 (C-11), 137.2 (C-4), 131.7 (C-10), 129.4 (C-1), 129.2 (C-7), 120.1 (C-5), 71.8 (C-8), 39.2 (C-3), 38.6 (C-9), 28.8 (C-6), 25.6 (C-2), 21.4 (C-12), 21.4 (C-13), 18.8 (C-14), 16.3 (C-15). EI-MS: 221.35[M+H⁺]. Anal. Calcd for C₁₅H₂₄O (220.18): C, 81.76; H, 10.98; O, 7.26. Found: C, 81.76; H, 10.95; O, 7.29.

(3*E*,7*E*)-3,7-dimethyl-10-(propan-2-ylidene)cyclodeca-3,7-dien-1-yl-acetate (3a) Yield: 67%, ¹H NMR (400 MHz, CDCl₃) δ 5.52 (dd, J = 5.8, 1.3 Hz, 1H), 5.31 (dd, J = 11.1, 9.6 Hz, 1H), 5.13 (dd, J = 11.3, 7.0 Hz, 1H), 2.54 (dd, J = 10.5, 6.5 Hz, 2H), 2.46 (dd, J = 15.8, 1.3 Hz,

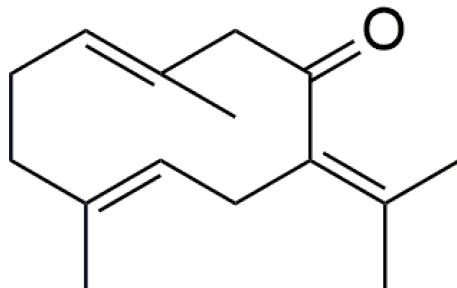


Figure 1: Structure of germacrone.

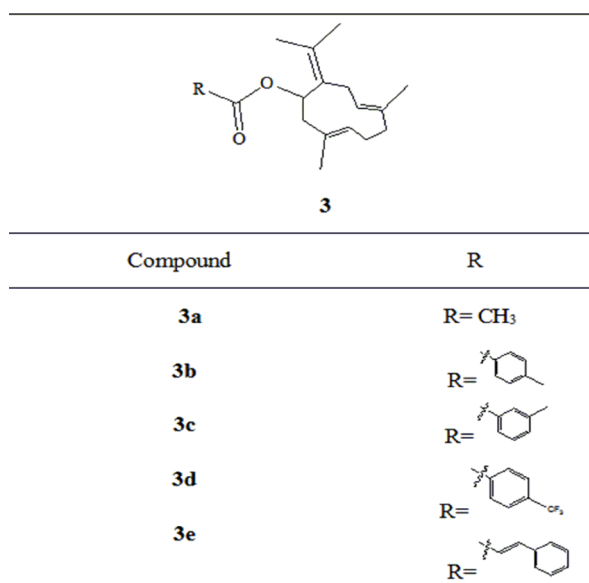


Figure 2: Germacrone derivatives.

1H), 2.39 (t, J = 4.2 Hz, 1H), 2.37 (d, J = 1.8 Hz, 1H), 2.35 (dd, J = 3.1, 1.6 Hz, 1H), 2.33 (t, J = 2.1 Hz, 1H), 2.31 (m, 1H), 2.10 (s, 3H), 1.77 (s, 6H), 1.58 (s, 3H), 1.55 (s, 3H). ¹³C NMR (100 MHz, (D₆) DMSO) δ 169.9 (C-16), 138.3 (C-11), 137.2 (C-4), 131.7 (C-10), 129.4 (C-1), 129.2 (C-7), 120.1 (C-5), 73.7 (C-8), 39.2 (C-3), 38.6 (C-9), 28.8 (C-6), 25.6 (C-2), 21.4 (C-12, C-13), 20.9 (C-17), 18.8 (C-14), 16.3 (C-15). EI-MS: 263.20 [M+H⁺]. Anal. Calcd for C₁₆H₂₄O₂ (262.19): C, 77.82; H, 9.99; O, 12.20. Found: C, 77.80; H, 9.98; O, 12.22.

(3E,7E)-3,7-dimethyl-10-(propan-2-ylidene)

cyclodeca-3,7-dien-1-yl-4-methylbenzoate (3b) Yield: 62%, ¹H NMR (400 MHz, CDCl₃) δ 7.92 (dd, J = 8.5, 1.7 Hz, 2H), 7.15 (dd, J = 8.5, 1.7 Hz, 2H), 5.54 (dd, J = 5.6, 1.6 Hz, 1H), 5.32 (dd, J = 11.1, 9.6 Hz, 1H), 5.17-5.09 (m, 1H), 2.55 (d, J = 10.0 Hz, 1H), 2.52 (d, J = 8.4 Hz, 1H), 2.43 (d, J = 1.9 Hz, 1H), 2.39 (s, 1H), 2.38 (s, 1H), 2.33 (s, 1H), 2.32 (d, J = 1.6 Hz, 3H), 2.32-2.30 (m, 2H), 1.77 (s, 6H), 1.58 (s, 3H), 1.57 (s, 3H). ¹³C NMR (100 MHz, (D₆) DMSO) δ 165.6 (C-16), 139.7 (C-20), 138.2 (C-11), 137.1 (C-4), 133.8 (C-17), 131.6 (C-10), 129.4 (C-1), 129.2 (C-7), 129.1 (C-18, C-22), 129 (C-19, C-21), 120.1 (C-5), 73.7 (C-8), 39.2 (C-3), 38.6 (C-9), 28.8 (C-6), 25.6 (C-2), 21.4 (C-12, C-13), 21.2 (C-23), 18.8 (C-14), 16.3 (C-15). EI-MS: 339.23[M+H⁺]. Anal. Calcd for C₂₃H₃₀O₂ (338.22): C, 81.61; H, 8.93; O, 9.45. Found: C, 81.61; H, 8.95; O, 9.43.

(3E,7E)-3,7-dimethyl-10-(propan-2-ylidene)

cyclodeca-3,7-dien-1-yl-3-methylbenzoate (3c) Yield: 47%, ¹H NMR (400 MHz, CDCl₃) δ 8.00-7.97 (m, 1H), 7.96 (s, 1H), 7.50 (t, J = 8.0 Hz, 1H), 7.40-7.35 (m, 1H), 5.54 (dd, J = 5.6, 1.6 Hz, 1H), 5.32 (dd, J = 11.3, 10.0 Hz, 1H), 5.16-5.09 (m, 1H), 2.56 (dd, J = 12.3, 10.5 Hz, 1H), 2.53-2.50 (m, 1H), 2.48-2.46 (m, 1H), 2.43 (d, J = 1.7 Hz, 3H), 2.39 (s, 1H), 2.38 (d, J = 3.7 Hz, 1H), 2.32 (d, J = 1.6 Hz, 1H), 2.32-2.25 (m, 2H), 1.77 (s, 6H), 1.58 (s, 3H), 1.57 (s, 3H). ¹³C NMR (100 MHz, (D₆) DMSO) δ 165.1 (C-16), 138.2 (C-11), 138.2 (C-19), 137.1 (C-4), 132.6 (C-22), 131.7 (C-10), 130.6 (C-18), 130.5 (C-20), 129.4 (C-1), 129.2 (C-7), 128.4 (C-21), 126.8 (C-17), 120.1 (C-

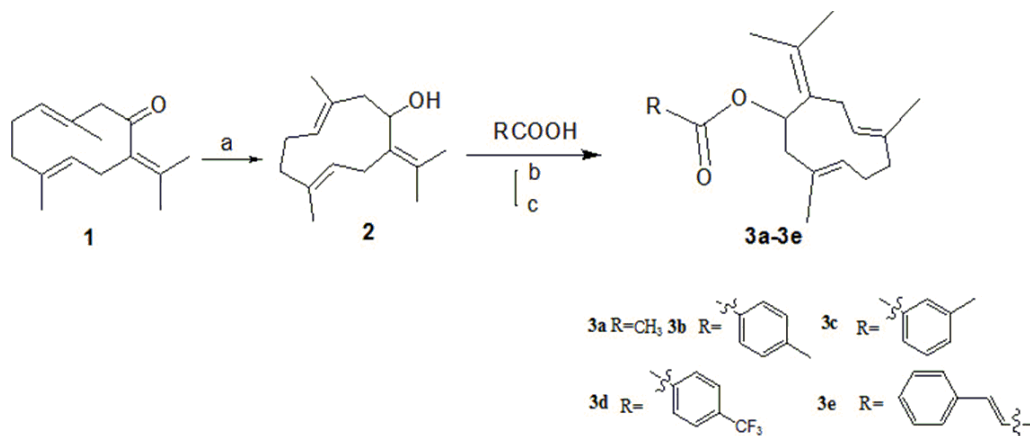
5), 73.7 (C-8), 39.2 (C-3), 38.6 (C-9), 28.8 (C-6), 25.6 (C-2), 21.4 (C-12, C-13), 20.9 (C-23), 18.8 (C-14), 16.3 (C-15). EI-MS: 339.26 [M+H⁺]. Anal. Calcd for C₂₃H₃₀O₂ (338.22): C, 81.61; H, 8.93; O, 9.45. Found: C, 81.62; H, 8.92; O, 9.45.

(3E,7E)-3,7-dimethyl-10-(propan-2-ylidene)

cyclodeca-3,7-dien-1-yl-4-(trifluoromethyl)benzoate (3d) Yield: 53%, ¹H NMR (400 MHz, CDCl₃) δ 7.95 (d, J = 8.6 Hz, 2H), 7.86 (d, J = 8.6 Hz, 2H), 5.53 (dd, J = 5.4, 1.9 Hz, 1H), 5.32 (dd, J = 11.0, 10.0 Hz, 1H), 5.16-5.09 (m, 1H), 2.57 (dd, J = 10.4, 8.6 Hz, 1H), 2.52 (dd, J = 10.3, 7.4 Hz, 1H), 2.44-2.39 (m, 1H), 2.39 (s, 1H), 2.38-2.34 (m, 2H), 2.32 (d, J = 1.6 Hz, 1H), 2.32-2.25 (m, 1H), 1.77 (s, 6H), 1.58 (s, 3H), 1.51 (s, 3H). ¹³C NMR (100 MHz, (D₆) DMSO) δ 165.6 (C-16), 138.3 (C-11), 137.2 (C-4), 133.8 (C-17), 132 (C-20), 131.6 (C-10), 129.4 (C-1), 129.2 (C-7), 129.1 (C-18, C-22), 125.1 (C-19, C-21), 124 (C-23), 120.1 (C-5), 73.7 (C-8), 39.2 (C-3), 38.6 (C-9), 28.8 (C-6), 25.6 (C-2), 21.4 (C-12, C-13), 18.8 (C-14), 16.3 (C-15). EI-MS: 393.20[M+H⁺]. Anal. Calcd for C₂₃H₂₇F₃O₂ (392.20): C, 70.39; H, 6.93; O, 8.15. Found: C, 70.39; H, 6.95; O, 8.15.

(Z)-(3E,7E)-3,7-dimethyl-10-(propan-2-ylidene)

cyclodeca-3,7-dien-1-yl-3-phenylacrylate (3e) Yield: 60%, ¹H NMR (400 MHz, CDCl₃) δ 7.66 (d, J = 16.4 Hz, 1H), 7.45 (dd, J = 6.5, 1.6 Hz, 1H), 7.44-7.40 (m, 2H), 7.40-7.35 (m, 2H), 6.69 (d, J = 16.1 Hz, 1H), 5.46 (dd, J = 5.6, 1.6 Hz, 1H), 5.32 (dd, J = 11.1, 9.6 Hz, 1H), 5.16-5.09 (m, 1H), 2.56 (dd, J = 13.1, 11.3 Hz, 1H), 2.53-2.48 (m, 1H), 2.43 (d, J = 1.6 Hz, 1H), 2.40-2.38 (m, 1H), 2.38-2.34 (m, 2H), 2.33 (d, J = 1.7 Hz, 1H), 2.32-2.25 (m, 1H), 1.77 (s, 6H), 1.58 (s, 3H), 1.53 (s, 3H). ¹³C NMR (100 MHz, (D₆) DMSO) δ 167 (C-16), 144.4 (C-18), 138.3 (C-11), 137.2 (C-4), 134.4 (C-19), 131.6 (C-10), 129.4 (C-1), 129.2 (C-7), 128.9 (C-22), 128.7 (C-21, C-23), 127.3 (C-20, C-24), 120.1 (C-5), 115.9 (C-17), 73.7 (C-8), 39.2 (C-3), 38.6 (C-9), 28.8 (C-6), 25.6 (C-2), 21.4 (C-12, C-13), 18.8 (C-14), 16.3 (C-15). EI-MS: 351.23[M+H⁺]. Anal. Calcd for C₂₄H₃₀O₂ (350.22): C, 82.24; H, 8.63; O, 9.13. Found: C, 82.22; H, 8.63; O, 9.15.



Scheme 1: Synthesis of 3a-3e.

Evaluation of biological activity

Biological activities were evaluated by investigating the effect of germacrone and its derivatives on HepG2, A549, Bel-7402 and HeLa cells. Cells were treated with compounds at the concentrations of 12.5 $\mu\text{mol/L}$, 25 $\mu\text{mol/L}$, 50 $\mu\text{mol/L}$, 100 $\mu\text{mol/L}$, 200 $\mu\text{mol/L}$, 400 $\mu\text{mol/L}$ and 800 $\mu\text{mol/L}$, respectively. MTT assay was then applied at 24 h, 48 h. As shown in Table 1. The proliferations of HepG2, Bel7402, A549 and HeLa cells were inhibited in a dose-dependent manner, and cytolytic activity was markedly inhibited at the same time. The growth-inhibitory effect had no significant differences after incubation with germacrone and derivatives for 24 h and 48 h (Figure 3), so there was no great influence to the anti-proliferation effect of germacrone and derivatives on Bel-7402, HepG2, A549 and HeLa cells with the extended treatment time after 24 h. However, all the compounds were active against Bel-7402, HepG2, A549 and HeLa cells to some extent. Inhibitions of germacrone derivatives (3a-3e) on these cells were stronger than germacrone and these results indicated that introduction of carboxylic esters could increase anticancer activity of germacrone, so we could elementary make sure that designed compounds should be well worth studying based on preliminary biological tests.

Compound 3b was found to show highest activity against HepG2 cell line with an IC_{50} value of 68.23 μM . Since references reported that germacrone induced apoptosis by inhibiting Bcl-2 expression and inducing p53 and Bax expression and induced cell cycle arrest and apoptosis through mitochondria-mediated caspase pathway, and induced apoptosis in human hepatoma HepG2 cells through inhibition of the JAK2/STAT3 signaling pathway [17–19]. Before we began to design these compounds, we carefully studied these references. Firstly, we hoped that designed compounds had stronger broad spectrum anti-tumor activities so we investigated their inhibitions on Bel-7402, HepG2, A549 and HeLa cells compared to germacrone. The results showed that these compounds, especially compound 3b had better effect on HepG2 cell than other cells. Then we investigated mechanism according to above-mentioned documents, but the pre-experimental results showed no effect reported in these references. Hu C T, et al., Wang SY, et al. and Xie B, et al. reported that HepG2 was inhibited by inhibiting c-Met/HGF signaling pathway. Because c-Met kinase is expressed in a number of cancers and our research area is major in finding novel c-Met inhibitors so we investigated inhibition of germacrone derivatives on c-Met kinase [20–22]. The results of compounds on c-Met kinase showed that germacrone derivatives were active

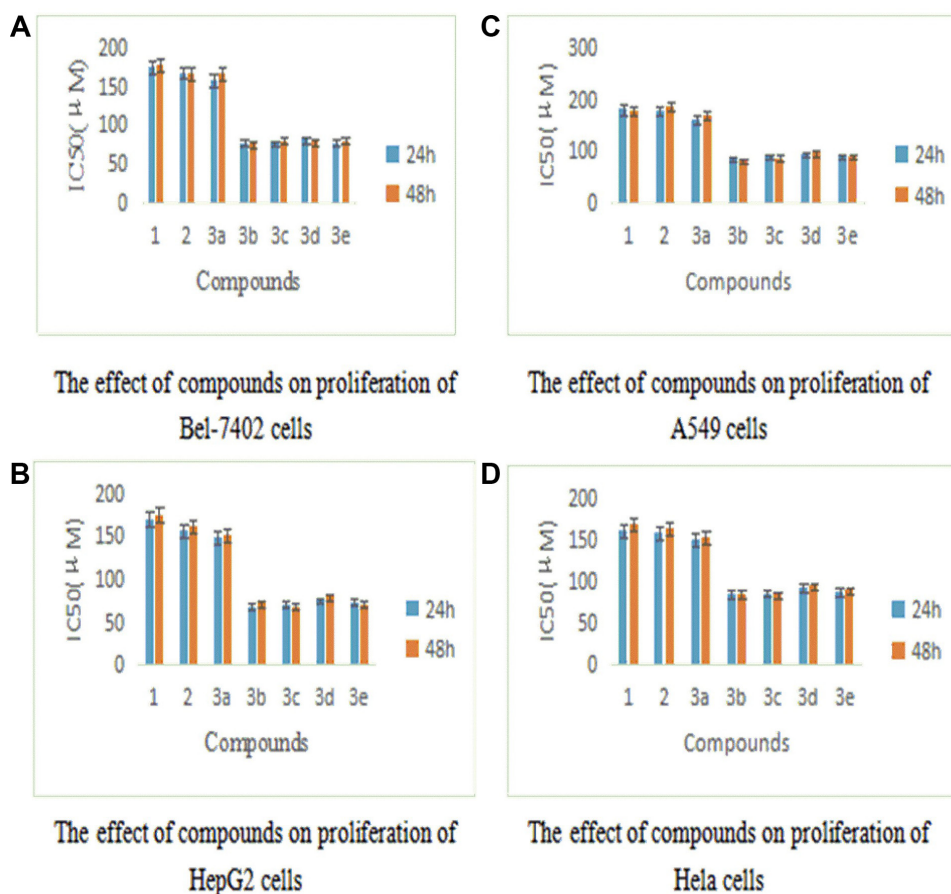


Figure 3: Inhibition of germacrone derivatives on Bel-7402, HepG2, A549 and HeLa cells.

Table 1: IC₅₀ values of compounds on Bel-7402, HepG2, A549 and Hela cells

Compound	Bel-7402 IC ₅₀ (μM)		HepG2 IC ₅₀ (μM)		A549 IC ₅₀ (μM)		Hela IC ₅₀ (μM)	
	24 h	48 h	24 h	48 h	24 h	48 h	24 h	48 h
1	173.54 ± 1.53	177.21 ± 1.97	169.52 ± 2.07	174.56 ± 1.88	179.97 ± 2.14	177.21 ± 1.87	160.69 ± 1.54	167.78 ± 1.81
2	167.08 ± 1.91	166.32 ± 1.83	155.2 ± 1.75	161.54 ± 1.32	177.21 ± 1.80	185.24 ± 1.99	157.31 ± 1.47	163.15 ± 1.73
3a	157.32 ± 1.33	166.25 ± 1.51	147.67 ± 1.47	151.59 ± 1.71	162.2 ± 1.55	168.87 ± 1.74	149.32 ± 1.33	152.95 ± 1.65
3b	75.85 ± 0.96	74.16 ± 0.83	68.23 ± 0.69	71.47 ± 0.82	84.85 ± 0.71	81.87 ± 0.88	83.64 ± 0.73	83.78 ± 0.76
3c	75.5 ± 1.05	78.55 ± 0.51	70.21 ± 0.87	67.84 ± 0.48	88.52 ± 0.53	87.21 ± 0.94	84.1 ± 0.71	82.54 ± 0.64
3d	80.14 ± 1.19	77.56 ± 0.77	74.66 ± 0.99	78.85 ± 0.77	93.48 ± 0.79	95.93 ± 0.97	91.25 ± 0.87	93.31 ± 0.90
3e	75.87 ± 0.81	79.22 ± 0.89	72.48 ± 0.64	69.98 ± 0.68	90.11 ± 0.75	88.21 ± 0.81	86.55 ± 0.80	88.24 ± 0.84

Table 2: IC₅₀ values of compounds against c-Met kinase

Compound	1	2	3a	3b	3c	3d	3e
IC ₅₀ (μM)	1.15	1.77	1.06	0.56	0.83	0.92	0.87

against c-Met kinase with IC₅₀ values of 1.06 μM, 0.56 μM, 0.83 μM, 0.92 μM, 0.87 μM, respectively (shown in Table 2). In accordance with the results of cells, the IC₅₀ values of 3a-3e were lower than germacrone, in which 3b had the best inhibitory effect with IC₅₀ value of 0.56 μM (Figure 4, Supplementary Table 1). The results suggested that derivatives had good activity so we could initially confirm that designed compounds might well repay investigation on the basis of preliminary activity tests. Further research works on activities are currently under investigation and will be reported in due course.

Docking studies

In pre-experiment, we carried out docking experiment by using several pdb proteins including 3DKF, 2WVG, 2RFS and 3DKC. Only 3DKC interacted with germacrone and derivatives owing to sesquiterpene structures and 3DKC was used frequently in our experiment so we chose it to make docking experiment. The 3DKC is the crystal structure of c-Met kinase in complex with ATP and its information is seen from <http://www.rcsb.org/pdb/explore/materialsAndMethods.do?structureId=3DKC>.

Docking experiments indicated that there was a binding mode between our synthesized compounds and the active site of protein 3dkc (shown in Figure 5). The (E, E)-1, 5-cyclodecadiene system interacted with the

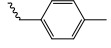
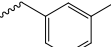
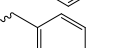
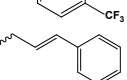
protein crystal 3dkc strongly by hydrophobic force and π-π stacking interaction of the benzene ring group. Compound 3b showed highest activity owing to hydrophobic interaction of methyl as shown in Figure 6. The binding energies were shown in Table 3. The compound 3b also had stronger binding energies and inhibition, in which R was methyl substituted benzene.

MD simulations and ΔGpred calculation

Molecular docking experiments gave a probably momentary binding mode that could be unreasonable and unstable. Molecular dynamics simulations were applied to perform further study of binding stabilities between compound (1-3e) and 3DKC. The crystal structures of 3DKC complex with 1-3e were used to evaluate the reliability of MD simulations. The RMSD curve and the surface area curve of the 1 ns indicated that 3b was relatively stable and the trajectories were well smoothly and other compounds were unstable with uneven trajectories (shown in Figure 7 and Supplementary Figure 1 to Supplementary Figure 7). The MD parameters were appropriate for the MD simulations.

The 2 3DKC-ligand complexes were performed by 8 ns MD simulations under identical MD conditions and all compounds gave stable RMSD curves during their MD simulations. ΔGpred were selected and ordered or 3DKC inhibitory activity assessment which values more negative than -25 kcal/mol. The predicted ΔGpred value of the 3b

Table 3: Binding energies of complexes between compounds and 3DKC

Compounds	R	c-Met Inhibition rate (%)	-CDOCKER energy (Kcal/mol)
1	-	27%	29.9587
2	-OH	23%	22.5548
3a	Me	31%	22.8715
3b		56%	65.2361
3c		47%	51.0112
3d		38%	40.1487
3e		41%	45.2356

compound was -28.36 kcal/mol while predicted ΔG_{pred} value of other compounds were more than -25 kcal/mol (shown in Table 4).

MATERIALS AND METHODS

Chemicals and reagents

All chemicals were obtained from Aladdin or J&K. Solvents were purified and dried by standard procedures, and stored over 3-Å molecular sieves. Reactions were followed by TLC using SILG/UV 254 silica-gel plates. Flash chromatography (FC): silica gel (SiO₂; 40 μm, 230-400 mesh). ¹H NMR and ¹³C NMR Spectra: Bruker Digital NMR Spectrometer, rep. δ in ppm, J in Hz. EI-MS: Waters ZQ4000. Cells were obtained from China Center for Type Culture Collection of Wuhan University; c-Met kinase were purchased from Millipore (Billerica, MA); RPMI-1640 culture medium and new-born calf serum from Gibco (Grand Island, NY); Methyl thiazolyl tetrazolium (MTT) was purchased from Amresco (Solon, OH).

Synthesis of compounds

Synthesis of 2

The suspension of LiAlH₄ (3.8 mg, 0.1 mmol) was added to a cold (-10°C) solution of 1 (21.8 mg, 0.1 mmol) in THF (15 ml) under argon and vigorous stirring. After 1 h (TLC control) the reaction was stopped by successive addition of water (2 drops), 6 N NaOH solution (2 drops) and water (4 drops). The mixture was extracted with DCM (3 × 20 ml) to give a crude product which was purified by silica gel column chromatography (hexane : t-butyl methyl ether, 70:30) to obtain 2 (18.3 mg, 84%).

Synthesis of 3a

A mixture of acetic acid (9 mg, 0.15 mmol), SOCl₂ (21.4 mg, 0.18 mmol), DMF 2 drops and DCM (5 ml) was refluxed for 4 h to obtain acetyl chloride. Acetyl chloride (11.8 mg, 0.15 mmol) was added portion wise to a solution of 2 (21.9 mg, 0.1 mmol), Py (15.8 mg, 0.2 mmol) in THF (15 ml) under nitrogen at 0°C. Then,

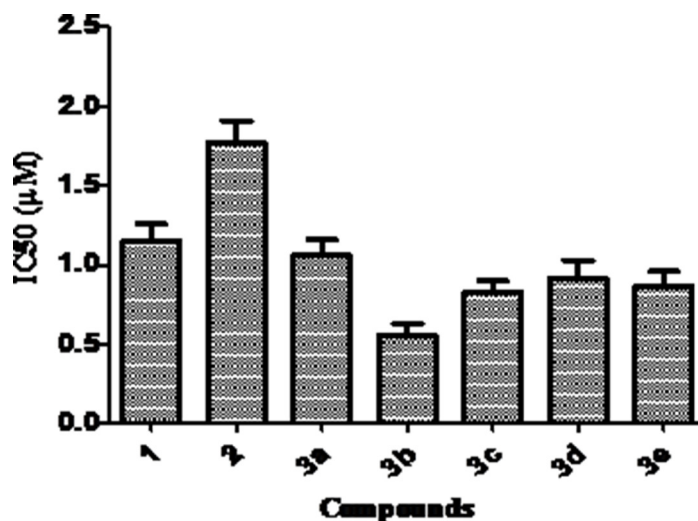
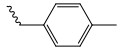
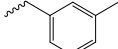
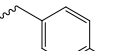
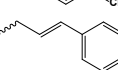


Figure 4: Inhibition of germacrone derivatives on c-Met kinase

Table 4: The value of -CDOCKER energy

Compounds	R	c-Met Inhibition rate (%)	-DeltaGpred Energy (kcal/mol)
1	-	27%	16.35
2	-OH	23%	12.31
3a	Me	31%	19.69
3b		56%	28.07
3c		47%	27.14
3d		38%	20.88
3e		41%	21.28

the mixture was stirred for 4 h at r.t. (TLC control), the solution was filtered. The solvent was removed under reduced pressure, and the crude product was purified by column chromatography (ethyl/acetat, 80/20) to obtain the target product 3a (17.4 mg, 67%).

Synthesis of 3b

A mixture of 2 (21.9 mg, 0.1 mmol), DMAP (6.1 mg, 0.05 mmol), para-toluic acid (13.6 mg, 0.1 mmol) and DCM (10 ml) was stirred for 30 min under nitrogen at -10°C , then, a solution of DCC (41.2 mg, 0.2 mmol) in DCM (5 ml) was added slowly and the mixture was stirred vigorously for 24 h at r.t. and filtered. The solvent was removed under reduced pressure to give a crude product which was purified by column chromatography to obtain the product 3b (20.8 mg, 62%).

Synthesis of 3c, 3d and 3e

Compounds 3c, 3d and 3e were prepared in analogy to 3b.

Cell culture

Bel-7402 cells, HepG2 cells (Human hepatoma cell line), A-549 and HeLa cells were investigated according to related reference [23] and the cells were cultured in RPMI 1640 and DMEM media supplemented with 10% FBS and

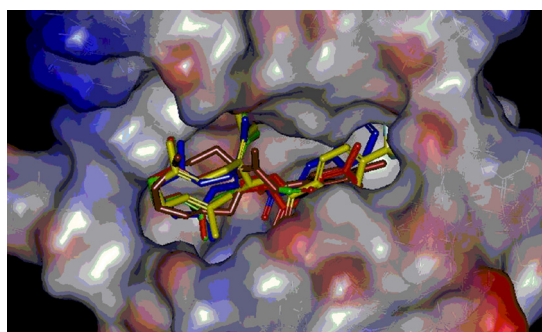
1%P/S (100 units/ml peni cillin and 100 mg/ml streptomycin), respectively, at 37°C in a 5% CO_2 atmosphere.

Cell assay

Proliferation of cells was evaluated by MTT assay [10]. Cells were inoculated at 1.0×10^4 cells/mL with 200 μL in each well of 96-well plate and allowed to adhere to the plates overnight. Then the cells were treated with a range of concentrations (0–800 $\mu\text{mol/L}$) of target products or 0.1% DMSO for 24, 48 h. 20 μL of MTT was added to each well and incubated at 37°C in dark for 4 h. After removal of the medium, cells were treated with 150 μL of DMSO and shaken for 15 min to completely dissolve the formazan crystals. The absorbances at 590 nm of the dissolved solutions were detected using a SpectraMAX190 microplate reader (Molecular Devices, USA).

Inhibition of c-Met kinase

The inhibitions of c-Met kinase were investigated referred to a published literature [24]. The IC_{50} values were detected using TR-FRET. 50 nM 6 His-tagged recombinant human c-Met residues 974-end (Millipore) was cultured in medium containing 2.5 m mol/L MnCl_2 , 10 m mol/L MgCl_2 , 20 m mol/L Tris, 2 m mol/L DTT and

**Figure 5: Compact binding modes of all compounds (PDB code: 3dke).**

0.01% Tween 20 with 5 m mol/L ATP and 200 n mol/L 5FAM-KKK -SPGEYVNIGFG-NH₂ with 25 μL at room temperature for 60 min. Compounds were made up to 100 μM solutions and were tested with 10 concentration gradients by two times dilutions. Each group was tested for three times Reactions were terminated by IMAP stop solution. Plates were incubated for an overnight and analyzed by using AlphaQuest.

Molecular docking

Molecular docking was performed according to related reference [25]. The docking experiment was carried out with CDOCKER program which was connected with Accelrys Discovery Studio 2.5.5. The programs adapted an empirical scoring function and a patented searching engine [26–27]. Briefly, ligands were docked into the corresponding

protein's binding site complied with protocol, which was generated by ligand from the crystal structure of 3DKC with random hydrogen atoms and GasteigerHückel charges but not water and ligands other parameters were default values except that the threshold was 1. The structure of receptor was minimized to 10,000 cycles using Powell method in DS 2.5.5. The geometries of all compounds were optimized by conjugate gradient method of TRIPOS. The convergence criterion was identified as 0.001 kcal/mol.

MD simulations

The MD simulations were performed on the basis of molecular docking by using AMBER 10.0 for ligands and AMBER ff03 for protein, and using Gaussian 03 program to calculate partial atomic charges at a neutral pH, with histidines 164 and 200 protonated at δ position,

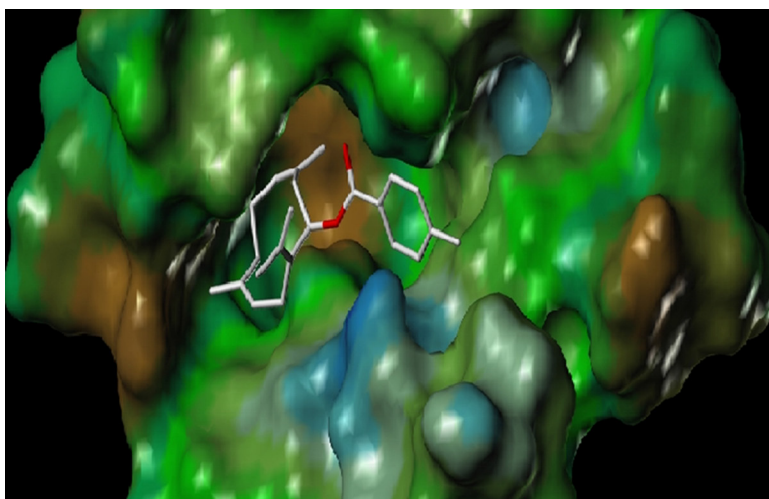


Figure 6: Conformation of 3b.

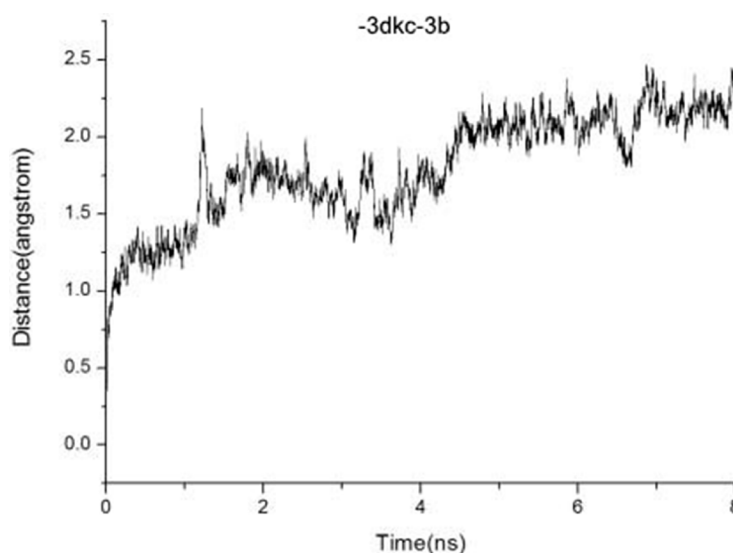


Figure 7: Plots of RMSD for all of the backbone atoms (Å) vs simulation time (ns) for 3DKC in complex with 3b.

and using SHAKE algorithm to restrict all the bonds given the time step of 2 fs and cutoff distance of 8 Å with long-range electrostatic interactions treated with the particle mesh Ewald (PME) method [28–30]. The heating operation was carried out from 0 to 300 K in 50 ps using Langevin dynamics at a constant volume and equilibrated for 100 ps at a constant pressure of 1 atm after four steps of minimizations, which included 2500 cycles of steepest descent minimization, followed by 2500 cycles of conjugated gradient minimization. Heavy atoms of receptor-ligand complex were restrained to 0, 10, 100, and 500 kcal/ (mol Å²) and were 10 kcal/ (mol Å²) during the heating and equilibration steps while solvent molecules were not restricted. Finally, periodic boundary conditions of 8 ns were performed for the whole system with normal pressure of 1 atm and normal temperature of 300 K in the production step.

MM-PBSA estimation of binding free energy ΔG_{pred}

For each system, ΔG_{pred} values were calculated using 100 snapshots recorded from the last with 1 ns trajectory an interval of 10 ps by Molecular Mechanics Poisson-Boltzmann Surface Area method [31–34].

CONCLUSIONS

The present study designed and synthesized novel compounds using germacrone as leading compound based on the combination principles. The results indicated that the major of compounds had moderate inhibition on cancer cells and c-Met kinase and introduction of carboxylic esters could increase anticancer activity of germacrone. These compounds can be further researched as antitumor leading structure and supply reference for developing anticancer with clinical value. The results of molecular docking and MD simulations were very important to explain molecular mechanism of eminent activities to c-Met kinase and binding stabilities between compounds and their receptors and these results can provide theoretical basis for further research c-Met inhibitors.

Abbreviations

DMSO, dimethyl sulfoxide; THF, tetrahydrofuran; DCC, dicyclohexylcarbodiimide; DMF, N, N-dimethyl formamide; DMAP, 4-dimethylaminopyridine; NMR, Nuclear Magnetic Resonance; TCL, thinlayer chromatography; DCM, dichloromethane; EI-MS, electron impact spectrometry; MTT, 3-(4, 5-dimethylthiazol-2-yl)-2,5-diphenyltetrazolium bromide.

CONFLICTS OF INTEREST

The authors declare no competing financial interest.

FUNDING

This study was supported by The Guangdong Strategic Emerging Project of Guangdong Provincial Department of Science and Technology (No. 2012A080800012), Special Fund of Applied Research and Development of Guangdong Provincial Department of Science and Technology (2015B020234009), Special Fund for TCM supported by State Administration of Traditional Chinese Medicine of China (201507004), The Joint Natural Sciences Fund of The Department of Science and Technology and The First Affiliated Hospital of Guangdong Pharmaceutical University (No.GYFYLH201317), Guangdong Natural Science Foundation (2015A030313586), and Science and Technology Planning Project of Guangdong Province (Guangdong Branch Regulations [2015]110). The authors are grateful to Mr Tan and Sun Yet-Sen University for molecular docking experiment.

REFERENCES

1. Chen W, Lu Y, Gao M, Wu J, Wang A, Shi R. Anti-angiogenesis effect of essential oil from *Curcuma zedoaria* *in vitro* and *in vivo*. *J Ethnopharmacol.* 2011; 133:220–26.
2. Matsuda H, Tewtrakul S, Morikawa T, Nakamura A, Yoshikawa M. Anti-allergic principles from Thai zedoary: structural requirements of curcuminoids for inhibition of degranulation and effect on the release of TNF- α and IL-4 in RBL-2H3 cells. *Bioorg Med Chem.* 2004; 12:5891–98.
3. Seo WG, Hwang JC, Kang SK, Jin UH, Suh SJ, Moon SK, Kim CH. Suppressive effect of *Zedoariae* rhizoma on pulmonary metastasis of B16 melanoma cells. *J Ethnopharmacol.* 2005; 101:249–57.
4. Chen CC, Chen Y, Hsi YT, Chang CS, Huang LF, Ho CT, Way TD, Kao JY. Chemical constituents and anticancer activity of *Curcuma zedoaria* roscoe essential oil against non-small cell lung carcinoma cells *in vitro* and *in vivo*. *J Agric Food Chem.* 2013; 61:11418–27.
5. Navarro DF, de Souza MM, Neto RA, Golin V, Niero R, Yunes RA, Delle Monache F, Cechinel Filho V. Phytochemical analysis and analgesic properties of *Curcuma zedoaria* grown in Brazil. *Phytomedicine.* 2002; 9:427–32.
6. Wilson B, Abraham G, Manju VS, Mathew M, Vimala B, Sundaresan S, Nambisan B. Antimicrobial activity of *Curcuma zedoaria* and *Curcuma malabarica* tubers. *J Ethnopharmacol.* 2005; 99:147–51.
7. Dang YY, Li XC, Zhang QW, Li SP, Wang YT. Preparative isolation and purification of six volatile compounds from essential oil of *Curcuma wenyujin* using high-performance centrifugal partition chromatography. *J Sep Sci.* 2010; 33:1658–64.
8. Cho W, Nam JW, Kang HJ, Windono T, Seo EK, Lee KT. Zedoarondiol isolated from the rhizoma of *Curcuma heyneana* is involved in the inhibition of iNOS, COX-2 and pro-inflammatory cytokines via the downregulation of NF- κ B pathway in LPS-stimulated murine macrophages. *Int Immunopharmacol.* 2009; 9:1049–57.

9. Xiao X, Zhao Y, Yuan H, Xia W, Zhao J, Wang X. [Study on the effect of *Rhizoma Curcuma Longa* on gastrin receptor]. [Article in Chinese]. *Zhong Yao Cai*. 2002; 25:184–85.
10. Liu Y, Wang W, Fang B, Ma F, Zheng Q, Deng P, Zhao S, Chen M, Yang G, He G. Anti-tumor effect of germacrone on human hepatoma cell lines through inducing G2/M cell cycle arrest and promoting apoptosis. *Eur J Pharmacol*. 2013; 698:95–102.
11. Schmidt L, Duh FM, Chen F, Kishida T, Glenn G, Choyke P, Scherer SW, Zhuang Z, Lubensky I, Dean M, Allikmets R, Chidambaram A, Bergerheim UR, et al. Germline and somatic mutations in the tyrosine kinase domain of the MET proto-oncogene in papillary renal carcinomas. *Nat Genet*. 1997; 16:68–73.
12. Ma PC, Kijima T, Maulik G, Fox EA, Sattler M, Griffin JD, Johnson BE, Salgia R. c-MET mutational analysis in small cell lung cancer: novel juxtamembrane domain mutations regulating cytoskeletal functions. *Cancer Res*. 2003; 63:6272–81.
13. Ma PC, Jagadeesh S, Jagadeeswaran R, Fox EA, Christensen J, Maulik G, Naoki K, Schaefer E, Lader A, Richards W, Sugarbaker D, Meyerson M, Salgia R. c-MET expression/activation, functions, and mutations in non-small cell lung cancer. *Cancer Res*. 2004; 64:430–431.
14. Di Renzo MF, Olivero M, Martone T, Maffè A, Maggiora P, Stefani AD, Valente G, Giordano S, Cortesina G, Comoglio PM. Somatic mutations of the MET oncogene are selected during metastatic spread of human HNSC carcinomas. *Oncogene*. 2000; 19:1547–55.
15. Lee JH, Han SU, Cho H, Jennings B, Gerrard B, Dean M, Schmidt L, Zbar B, Vande Woude GF. A novel germ line juxtamembrane Met mutation in human gastric cancer. *Oncogene*. 2000; 19:4947–53.
16. Feng Y, Thiagarajan PS, Ma PC. MET signaling: novel targeted inhibition and its clinical development in lung cancer. *J Thorac Oncol*. 2012; 7:459–67.
17. Xie XH, Zhao H, Hu YY, Gu XD. Germacrone reverses Adriamycin resistance through cell apoptosis in multidrug-resistant breast cancer cells. *Exp Ther Med*. 2014; 8:1611–15.
18. Zhong Z, Chen X, Tan W, Xu Z, Zhou K, Wu T, Cui L, Wang Y. Germacrone inhibits the proliferation of breast cancer cell lines by inducing cell cycle arrest and promoting apoptosis. *Eur J Pharmacol*. 2011; 667:50–55.
19. Liu YY, Zheng Q, Fang B, Wang W, Ma FY, Roshan S, Banafa A, Chen MJ, Chang JL, Deng XM, Li KX, Yang GX, He GY. Germacrone induces apoptosis in human hepatoma HepG2 cells through inhibition of the JAK2/STAT3 signalling pathway. *J Huazhong Univ Sci Technolog Med Sci*. 2013; 33:339-45.
20. Hu CT, Cheng CC, Pan SM, Wu JR, Wu WS. PKC mediates fluctuant ERK-paxillin signaling for hepatocyte growth factor-induced migration of hepatoma cell HepG2. *Cell Signal*. 2013; 25:1457–67.
21. Wang SY, Chen B, Zhan YQ, Xu WX, Li CY, Yang RF, Zheng H, Yue PB, Larsen SH, Sun HB, Yang X. SU5416 is a potent inhibitor of hepatocyte growth factor receptor (c-Met) and blocks HGF-induced invasiveness of human HepG2 hepatoma cells. *J Hepatol*. 2004; 41:267–73.
22. Xie B, Tang C, Chen P, Gou YB, Xiao J, Du H. [The effect of hepatitis B virus X protein on the c-met promoter activity in HepG2 cells]. [Article in Chinese]. *Zhonghua Gan Zang Bing Za Zhi*. 2009; 17:292–96.
23. Chen W, Liu Y, Li M, Mao J, Zhang L, Huang R, Jin X, Ye L. Anti-tumor effect of α -pinene on human hepatoma cell lines through inducing G2/M cell cycle arrest. *J Pharmacol Sci*. 2015; 127:332–38.
24. Buchanan SG, Hendle J, Lee PS, Smith CR, Bounaud PY, Jessen KA, Tang CM, Huser NH, Felce JD, Froning KJ, Peterman MC, Aubol BE, Gessert SF, et al. SGX523 is an exquisitely selective, ATP-competitive inhibitor of the MET receptor tyrosine kinase with antitumor activity *in vivo*. *Mol Cancer Ther*. 2009; 8:3181–90.
25. Ye L, Tian Y, Li Z, Jin H, Zhu Z, Wan S, Zhang J, Yu P, Zhang J, Wu S. Design, synthesis and molecular docking studies of some novel spiro[indoline-3, 4'-piperidine]-2-ones as potential c-Met inhibitors. *Eur J Med Chem*. 2012; 50:370–75.
26. Jain AN. Surflex: fully automatic flexible molecular docking using a molecular similarity-based search engine. *J Med Chem*. 2003; 46:499–511.
27. Jain AN. Surflex-Dock 2.1: robust performance from ligand energetic modeling, ring flexibility, and knowledge-based search. *J Comput Aided Mol Des*. 2007; 21:281–306.
28. Vay JL, Fawley W. AMBER User's Manual. Interim Report. 2008; 3:22–5.
29. Frisch MJ, Trucks GW, Schlegel HB, et al. Gaussian 03, Revision E.01; Gaussian, Inc.: Pittsburgh PA. 2004.
30. Miyamoto S, Kollman PA. Settle: an analytical version of the SHAKE and RATTLE algorithm for rigid water models. *J Comput Chem*. 1992; 13:952–62.
31. Massova I, Kollman PA. Combined molecular mechanical and continuum solvent approach (MM-PBSA/GBSA) to predict ligand binding. *Perspect Drug Discov Des*. 2000; 18:113–15.
32. Hou T, Wang J, Li Y, Wang W. Assessing the performance of the MM/PBSA and MM/GBSA methods. 1. The accuracy of binding free energy calculations based on molecular dynamics simulations. *J Chem Inf Model*. 2011; 51:69–82.
33. Liu M, Yuan M, Luo M, Bu X, Luo HB, Hu X. Binding of curcumin with glyoxalase I: molecular docking, molecular dynamics simulations, and kinetics analysis. *Biophys Chem*. 2010; 147:28–34.
34. He L, He F, Bi H, Li J, Zeng S, Luo HB, Huang M. Isoform-selective inhibition of chrysin towards human cytochrome P450 1A2. Kinetics analysis, molecular docking, and molecular dynamics simulations. *Bioorg Med Chem Lett*. 2010; 20:6008–12.